

MOL #79699

Virtual Screening for LPA₂-Specific Agonists Identifies a Nonlipid Compound with Antiapoptotic Actions

Gyöngyi N. Kiss, James I. Fells, Renuka Gupte, Sue-Chin Lee, Jianxiong Liu, Nóra Nusser, Keng G. Lim, Ramesh M. Ray, Fang-Tsyr Lin, Abby L. Parrill, Balázs Sümegi, Duane D. Miller, Gabor Tigyi

Department of Physiology, University of Tennessee Health Science Center, Memphis TN, USA

Affiliations

Department of Physiology, University of Tennessee Health Science Center, Memphis, TN, USA - GNK, JIF, SCL, JL, NN, KGL, RMR

Department of Biochemistry and Medical Chemistry, University of Pécs, Pécs, Hungary - GNK, BS

Department of Pharmaceutical Sciences, University of Tennessee Health Science Center, Memphis, TN, USA - RG, DMD

Department of Medicine, Section of Hematology/Oncology, Baylor College of Medicine, Houston, TX, USA - FTL

ALP - Computational Research on Materials Institute, Department of Chemistry, University of Memphis, TN, USA

MOL #79699

Running Title: Nonlipid LPA₂-specific agonist with antiapoptotic action

Address correspondence to:

Gabor Tigyi, M.D., Ph.D.

Department of Physiology, UTHSC

894 Union Avenue

Memphis TN 38163

Tel.: 901-448-4793

Fax: 901-448-7126

Email: gtigyi@uthsc.edu

Number of text pages: 44

Number of tables: 2

Number of figures: 9

Number of references: 51

Number of words in the Abstract: 249

Number of words in the Introduction: 727

Number of words in the Discussion: 1,514

MOL #79699

Nonstandard abbreviations

Akt, protein kinase B; ATX, autotaxin; B103, rat neuroblastoma cells; Bax, Bcl-2-associated X protein; Bcl-2, B-cell lymphoma 2; BSA, bovine serum albumin; CHO, Chinese hamster ovary; CHX, cycloheximide; DKO, double knockout; DMEM, Dulbecco's modified Eagle medium; DMSO, dimethyl sulfoxide; EDG, endothelial differentiation gene; EGFP, enhanced green fluorescent protein; ERK1/2, extracellular signal regulated kinases 1/2; FBS, fetal bovine serum; Fura-2AM, Fura-2-acetoxymethyl ester; GPCR, G protein-coupled receptor; GRI, Genome Research Institute; H2L, Hit2Lead; HUVEC, human umbilical vein endothelial cells; IEC-6, intestinal epithelial cell line 6; LPA, lysophosphatidic acid; LPAR, LPA receptor; MEF, mouse embryonic fibroblast; MM1, rat hepatoma cells; MMFF94, Merck Molecular Force Field 94; MMP, matrix metalloproteinase; NF κ B, nuclear factor κ B; NHERF2, Na⁺-H⁺ exchange regulatory factor 2; OTP, octadecenyl thiophosphate; PARP-1, poly (ADP-ribose) polymerase 1; PBS, phosphate-buffered saline; PDZ, PSD95/Dlg/ZO-1 domain; RH7777, McArdle rat hepatoma cell line; S1P, sphingosine-1-phosphate; TM, transmembrane; TNF- α , tumor necrosis factor α ; TRIP6, thyroid receptor interacting protein 6; UC-DDC, University of Cincinnati Drug Discovery Center; uPA, urokinase.

MOL #79699

ABSTRACT

Lysophosphatidic acid (LPA) is a highly potent endogenous lipid mediator that protects and rescues cells from programmed cell death. Earlier work identified the LPA₂ G protein-coupled receptor subtype as an important molecular target of LPA mediating the antiapoptotic signaling. Here we describe the results of a virtual screen using single-reference similarity searching that yielded compounds NSC12404, GRI977143, H2L5547924, and H2L5828102, novel nonlipid and drug-like hits that are specific for the LPA₂ receptor subtype. We characterized the antiapoptotic action of one of these hits GRI977143 that was effective in reducing activation of caspases 3, 7, 8, and 9 and inhibited poly (ADP-ribose) polymerase 1 cleavage and DNA fragmentation in different extrinsic and intrinsic models of apoptosis in vitro. Furthermore, GRI977143 promoted carcinoma cell invasion of human umbilical vein endothelial cell monolayers and fibroblast proliferation. The antiapoptotic cellular signaling responses were present selectively in mouse embryonic fibroblast cells derived from LPA_{1&2} double knockout mice reconstituted with the LPA₂ receptor and were absent in vector-transduced control cells. GRI977143 was an effective stimulator of extracellular signal regulated kinases 1/2 activation and promoted the assembly of a macromolecular signaling complex consisting of LPA₂, Na⁺-H⁺ exchange regulatory factor 2, and thyroid receptor interacting protein 6, which has been shown previously as a required step in LPA-induced antiapoptotic signaling. The present findings indicate that nonlipid LPA₂-specific agonists represent an excellent starting point for development of lead compounds with potential therapeutic utility for preventing the programmed cell death involved in many types of degenerative and inflammatory diseases.

MOL #79699

INTRODUCTION

The growth factor-like lysophospholipids lysophosphatidic acid (LPA) and sphingosine-1-phosphate (S1P) regulate many fundamental cellular responses, ranging from cell survival through cell proliferation to cell motility and migration (Tigyi, 2010). To date, specific inhibitors of the LPA and S1P receptors have taken center stage in drug discovery efforts. The functional antagonist of S1P receptors fingolimod (Brinkmann et al., 2010) has been recently approved by the Food and Drug Administration (FDA) for the first-line treatment of multiple sclerosis; and AM152 (Swaney et al., 2011), an LPA₁-selective antagonist has been granted orphan drug status for the treatment of fibrotic diseases. A decade ago, we had already shown that LPA has profound activity in preventing apoptosis and can also rescue apoptotically condemned cells from the progression of the apoptotic cascade (Deng et al., 2002; Deng et al., 2004; Deng et al., 2007; Deng et al., 2003). We developed an LPA mimic, octadecenyl thiophosphate (OTP) (Durgam et al., 2006), which has superior efficacy compared to LPA in vitro and in vivo in rescuing cells and animals from radiation-induced apoptosis (Deng et al., 2007). Development of LPA-based drug candidates has been limited to the discovery of lipid-like ligands, which is understandable due to the hydrophobic environment of the S1P and LPA G protein-coupled receptor (GPCR) ligand binding pockets (Fujiwara et al., 2007; Hanson et al., 2012; Li et al., 2005; Parrill et al., 2000; Valentine et al., 2008; Wang et al., 2001). Only a few LPA receptor ligands break away from lipid-like structural features, among which Ki16425, an LPA_{1/2/3} antagonist (Ohta et al., 2003), and the AM095-152 series of LPA₁-selective compounds are of importance (Swaney et al., 2011).

MOL #79699

In order to exploit the potential therapeutic benefits of LPA, discovery and development of drug-like nonlipid compounds might be beneficial. In the present study, we applied virtual screening strategies using similarity searching that we derived from the previously validated molecular models of these receptors, and we limited our searches to chemical libraries with drug-like compounds that satisfy Lipinski's rule of five (Lipinski, 2003). We focused our virtual screen on the discovery of ligands for the LPA₂ receptor subtype because of our long-standing interest in developing compounds that can attenuate programmed cell death elicited by radiation and chemotherapy. The choice of this receptor subtype is based on mounting evidence that LPA₂ is unique among this class of receptors in its ability to initiate signaling events that promote cell survival and prevent the progression of apoptosis (Deng et al., 2007; E et al., 2009; Lin et al., 2007). This objective was further fueled by our recent successes with OTP (Deng et al., 2007). Our objective in the present study was to identify nonlipid LPA₂ agonist scaffolds that can lead to the development of new drug candidates capable of alleviating the side effects of chemo- and radiation treatment of cancer patients and potentially function as radiomitigators against lethal levels of radiation injury.

Here we report on the identification of four nonlipid compounds that are specific agonists of LPA₂. We selected one of these hits GRI977143 [2-((3-(1,3-dioxo-1*H*-benzo[de]isoquinolin-2(3*H*)-yl)propyl)thio)benzoic acid] from the Genome Research Institute (GRI) chemical library and characterized its cellular, pharmacological and signaling responses in several assay systems. Our results show that the compound GRI977143 is a specific agonist of LPA₂ and does not activate any other known or putative LPA GPCR. We also show that GRI977143 is similarly effective compared to

MOL #79699

LPA and OTP in preventing programmed cell death, although in Ca^{2+} -mobilization and caspase 3 and 7 inhibition assays it has higher EC_{50} values than the other two ligands. GRI977143 inhibited activation of caspases 3, 7, 8, and 9, B-cell lymphoma 2 (Bcl-2)-associated X protein (Bax) translocation, and poly (ADP-ribose) polymerase 1 (PARP-1) cleavage, leading to reduced DNA fragmentation following activation of the extrinsic or intrinsic apoptotic signaling cascades. We also provide evidence that GRI977143 robustly activates the extracellular signal regulated kinases 1/2 (ERK1/2) survival pathway and leads to the assembly of a macromolecular signalosome consisting of LPA_2 , thyroid receptor interacting protein 6 (TRIP6), and Na^+ - H^+ exchange regulatory factor 2 (NHERF2), which has been shown to be required for the prosurvival signaling elicited via this receptor subtype. GRI977143 and the three other nonlipid hits NSC12404 [2-((9-oxo-9*H*-fluoren-2-yl)carbamoyl)benzoic acid], H2L5547924 [4,5-dichloro-2-((9-oxo-9*H*-fluoren-2-yl)carbamoyl)benzoic acid], and H2L5828102 [2-((9,10-dioxo-9,10-dihydroanthracen-2-yl)carbamoyl)benzoic acid] described in this paper represent a good starting point for lead development and optimization, which may yield novel LPA-based drug candidates for therapeutic applications.

MOL #79699

MATERIALS AND METHODS

Materials

Lysophosphatidic acid (18:1) was purchased from Avanti Polar Lipids (Alabaster, AL). OTP was synthesized and provided by RxBio, Inc. (Johnson City, TN) as described (Durgam et al., 2006). The test compounds used in the present study were obtained from the following vendors: Genome Research Institute (GRI) GRI977143 from the University of Cincinnati Drug Discovery Center (UC-DDC; Cincinnati, OH); Hit2Lead (www.hit2lead.com) H2L5547924, and H2L5828102, from ChemBridge (San Diego, CA); and NSC12404 from the National Cancer Institute Developmental Therapeutics Program Open Chemical Repository. Ten mM stock solutions of GRI977143, H2L5547924, H2L5828102, and NSC12404 were prepared in dimethyl sulfoxide (DMSO). One millimolar stocks of LPA and OTP as an equimolar complex of charcoal-stripped, fatty acid-free bovine serum albumin (BSA) (Sigma-Aldrich) St. Louis, MO) were prepared just before use in phosphate-buffered saline (PBS). A stock solution of 3.45 mM Adriamycin was prepared in distilled water.

Computational docking

Compounds were flexibly docked into the activated LPA₂ receptor homology model reported by Sardar et al. (Sardar et al., 2002) using Autodock Vina (Trott and Olson, 2010). The compounds and receptor homology model were both energy optimized with the Merck Molecular Force Field 94 (MMFF94) in the Molecular Operating Environment software (MOE, 2002) prior to docking. Docking simulations were performed using a

MOL #79699

docking box with dimensions of 65 x 63 X 50 Å and a search space of 20 binding modes, and an exhaustive search parameter was set at 5. The best docking pose was chosen based on the lowest energy conformation. Finally, the best pose was further refined using the MMFF94 in MOE.

Ligand-based similarity search

Similarity searching of NSC12404 was performed using the UC-DDC library database (drugdiscovery.uc.edu). The Tanimoto similarity indices for the reference compounds were calculated using ECFC6, FCFP4, and FCFP6 fingerprints in Pipeline Pilot software (Accelrys, Inc.; San Diego, CA). The UC-DCC library was screened using Pipeline Pilot fingerprints to identify additional LPA₂ ligands. A similarity threshold was set at 80%. Among the 225 returned hits, compounds with similarity > 80% were selected by visual inspection, carefully considering the similarity and how closely the structures reflected the reference compound. A total of 27 compounds was selected for evaluation using LPA receptor-activated Ca²⁺-mobilization assays.

Residue nomenclature

Amino acids in the transmembrane (TM) domains were assigned index positions to facilitate comparison between GPCRs with different numbers of amino acids, as described by Ballesteros and Weinstein (Ballesteros, 1995). An index position is in the format X.YY., where X denotes the TM domain in which the residue appears, and YY indicates the position of that residue relative to the most highly conserved residue in that TM domain, which is arbitrarily assigned position 50.

MOL #79699

LPA receptor-mediated Ca²⁺ mobilization assay

Stable cell lines expressing the individual LPA₁, LPA₂, LPA₃, LPA₄, and LPA₅ established receptor subtypes (Tigyi, 2010), as well as putative LPA receptors GPR87 (Tabata et al., 2007) and P2Y10 (Murakami et al., 2008), or appropriate empty vector-transfected controls have been previously generated and described (Murakami et al., 2008; Tabata et al., 2007; Williams et al., 2009). Assays for ligand-activated mobilization of intracellular Ca²⁺ were performed using a Flex Station 2 robotic fluorescent plate reader (Molecular Devices; Sunnyvale, CA) as previously described (Durgam et al., 2006). The appropriate concentrations of the test compounds were either used alone (for agonist testing) or mixed with the respective ~EC₇₅ concentration of LPA 18:1 for the LPA receptor being tested (antagonist screen). The cells were loaded with Fura -2-acetoxymethyl ester (Fura-2/AM) in Krebs buffer containing 0.01% pluronic acid for 30 min and rinsed with Krebs buffer before measuring Ca²⁺ mobilization. The ratio of peak emissions at 510 nm after 2 min of ligand addition was determined for excitation wavelengths of 340 nm/380 nm. All samples were run in quadruplicate. The inhibition elicited by 10 μM test compound on the EC₇₅ concentration of LPA 18:1 for a given receptor (I_{10μM}) was interpolated from the dose-response curves. The half maximally effective concentration (EC₅₀), and inhibitory constant (K_i) values were calculated by fitting a sigmoid function to dose-response data points using the Prism 5 software (GraphPad Software, Inc., La Jolla, CA, USA).

Cell culture

MOL #79699

Mouse embryonic fibroblast (MEF) cells were isolated from E13.5 LPA_{1&2} double knockout (DKO) embryos (Lai et al., 2007). MEFs were transduced with empty vector or LPA₂-containing lentiviruses and selected with 1.5 µg/ml puromycin. Cells were maintained in Dulbecco's modified Eagle medium (DMEM) supplemented with 10% (V/V) fetal bovine serum (FBS), 2 mM L-glutamine, 100 U/mL penicillin, and 100 µg/mL streptomycin. Serum-free medium contained 0.1% (W/V) BSA in DMEM. The rat intestinal epithelial cell line 6 (IEC-6) was obtained from the American Type Culture Collection (Rockville, MD) at passage 13; passages 16–21 were used in all experiments. IEC-6 cells were maintained in a humidified 37 °C incubator in an atmosphere of 90% air and 10% CO₂. Growth medium consisted of DMEM supplemented with 5% heat inactivated FBS, 10 µg/mL insulin, and 50 µg/mL gentamycin. The composition of the serum-starvation medium was the same as that of the full growth medium except that it contained no FBS. The McArdle rat hepatoma cell line (RH7777) stably expressing LPA₂ receptors was a gift from Dr. Fumikazu Okajima (Gunma University, Maebashi, Japan). RH7777 cells stably expressing LPA₁ or LPA₃ receptors were generated in-house and characterized earlier (Fischer et al., 2001). Wild type and LPA receptor (LPAR) stably transfected RH7777 cells were grown in DMEM supplemented with 10% FBS and 2 mM L-glutamine in the presence of 250 µg/ml G418. Chinese hamster ovary (CHO) cells stably expressing either vector or LPA₄ receptor were a kind gift from Dr. Takao Shimizu (Tokyo University; Tokyo, Japan). Cells were cultured in Ham's F12 medium containing 10% FBS, 2 mM L-glutamine, and 350 µg/ml G418. Rat neuroblastoma cells (B103) were transduced with the lentivirus harboring wild type of FLAG-LPA₅ and selected with puromycin to

MOL #79699

establish the stable cell lines. The stable cells were maintained in DMEM supplemented with 10% FBS and 0.4 $\mu\text{g/ml}$ puromycin. GPR87- and P2Y10-expressing CHO cells and vector-transfected control cells were a gift from Dr. Norihisha Fujita (Ritsumeikan University; Shiga, Japan). The highly invasive MM1 rat hepatoma cells (gift from Dr. Michiko Mukai, Osaka University, Japan) were grown in suspension in DMEM supplemented with 10% (V/V) FBS, 2 mM L-glutamine, 100 U/mL penicillin, and 100 $\mu\text{g/mL}$ streptomycin. Human umbilical vein endothelial cells (HUVEC) were purchased from VEC Technologies Inc. (Rensselaer, NY, USA) and cultured in MCDB-131 complete medium supplemented with 10% (V/V) FBS, 90 $\mu\text{g/mL}$ heparin, 10 ng/mL EGF, 1 $\mu\text{g/mL}$ hydrocortisone, 0.2 mg/mL EndoGrowth (VEC Technologies Inc.) supplement, 100 U/mL penicillin G, 100 $\mu\text{g/mL}$ streptomycin, and 25 $\mu\text{g/mL}$ amphotericin B.

Cell proliferation assay

For determination of the effect of the LPA receptor ligands on cell growth, vector- and LPA₂-transduced MEF cells (2×10^4) were plated in each well of a 24-well plate in full growth medium. Cells were counted the next day and the medium was replaced with medium containing 1.5% (V/V) FBS supplemented with or without 1 μM LPA, 1 μM OTP, or 10 μM GRI977143. Media containing LPA, OTP, and GRI977143 were refreshed every 24 h. The growth rate was measured by counting the number of cells in triplicate using the Z1 Coulter Particle Counter (Beckman Coulter; Hialeah, FL) as a function of time.

Induction of apoptosis by Adriamycin or serum withdrawal

MOL #79699

Experiments were performed on vector- and LPA₂-transduced MEF cells. To measure caspase 3, 7, 8, or 9 activity and DNA fragmentation, cells were plated in 48-well plates (2×10^4 cells/well). To detect PARP-1 cleavage and Bax translocation, 1.5×10^6 cells were plated in 10-cm dishes and cultured overnight in full growth medium. The next morning, the growth medium was replaced by serum-starvation medium and cells were pretreated for 1 h with LPA (1-10 μ M), OTP (1-10 μ M), GRI977143 (1-10 μ M), or vehicle. Caspase activity, DNA fragmentation, PARP-1 cleavage, and Bax translocation were measured 5 h after incubation with 1.7 μ M Adriamycin or 24 h after serum withdrawal.

Induction of apoptosis by tumor necrosis factor α (TNF- α) in IEC-6 cells

Confluent serum-starved IEC-6 cells were treated with or without TNF- α (10 ng/ml)/cycloheximide (CHX) (20 μ g/ml) (Deng et al., 2002) in the presence of OTP (10 μ M), GRI977143 (10 μ M), or LPA (1 μ M) for 3 h. Cells were washed twice with PBS and the quantitative DNA fragmentation assay was carried out as described previously (Valentine et al., 2010).

Caspase activity assay

Caspase-Glow^R 3/7, Caspase-Glow^R 8 and Caspase-Glow^R 9 reagents were purchased from Promega (Madison, WI) and used according to the manufacturer's instructions. Briefly, cells were lysed by adding 50 μ l of lysis reagent per well, followed by shaking for 30 min at room temperature. Two hundred μ l lysate were transferred to a 96-well white-

MOL #79699

wall plate, and luminescence was measured using a BioTek (Winooski, VT) plate reader.

DNA fragmentation ELISA

Apoptotically-challenged cells were washed twice with PBS, and a quantitative DNA fragmentation assay was carried out using a Cell Death Detection ELISA PLUS kit (Roche Diagnostics, Penzberg, Germany) and normalized to protein concentration using the BCA Protein Assay Kit (Thermo Fisher Scientific, Inc.; Rockford, IL) as described previously (Valentine et al., 2010). Aliquots of nuclei-free cell lysate were placed in streptavidin-coated wells and incubated with anti-histone-biotin antibody and anti-DNA peroxidase-conjugated antibody for 2 h at room temperature. After the incubation, the sample was removed, and the wells were washed and incubated with 100 μ l 2,2'-azino-di[3-ethylbenzthiazolin-sulfonate substrate at room temperature before the absorbance was read at 405 nm. Results were expressed as absorbance at 405 nm/min/mg protein as detailed in our previous report (Ray et al., 2011).

MM1 hepatoma cell invasion of endothelial monolayer

HUVEC (1.3×10^5 cells at passages 5 to 7) were seeded into each well of a 12-well plate pre-coated with 0.2% gelatin (Sigma-Aldrich). Cells were grown for two days until a confluent monolayer was formed. MM1 cells were pre-labeled with 2 μ g/mL calcein AM (Life Technologies; Grand Island, NY) for 2 h and rinsed twice, and 5×10^4 cells per well were seeded over the HUVEC monolayer. Tumor-monolayer cell invasion was carried out for 20 h in MCDB-131 complete media containing 1% FBS with or without

MOL #79699

the addition of 1 μM LPA or 1-10 μM GRI977143. Non-invaded tumor cells were removed by repeatedly rinsing the monolayer with PBS (containing Ca^{2+} and Mg^{2+}), followed by fixation with 10% buffered formalin. Tumor cells that penetrated the monolayer were photographed using a NIKON TiU inverted microscope with phase-contrast and fluorescence illumination. The fluorescent and phase-contrast images were overlaid using Elements BR software (Nikon, version 3.1x). A total of five non-overlapping fields was imaged per well, and the number of invaded MM1 cells (displaying a flattened morphology underneath the monolayer) was counted.

Immunoblot analysis

To detect ligand-induced ERK1/2 activation, vector- and LPA₂-transfected MEF cells were serum starved 3 h before exposure to 1 μM LPA, 1 μM OTP, 10 μM GRI977143, or vehicle for 10 min. For ERK1/2 activation and PARP-1 cleavage measurements, cells were harvested in 1X Laemmli sample buffer and separated using 12% Laemmli SDS-polyacrylamide gels. To assess Bax translocation, cell lysates were separated into cytosolic, mitochondrial, and nuclear fractions using the Cell Fractionation Kit-Standard (MitoSciences; Eugene, OR). Cytosolic fractions were then concentrated by precipitation with 75% trichloroacetic acid, and the pellets were dissolved in 50 mM non-neutralized Tris pH 10 buffer and 6X Laemmli buffer. Samples were boiled for 5 min and loaded onto 12% SDS-polyacrylamide gels. Western blotting was carried out as previously described (Valentine et al., 2010). Primary antibodies against pERK1/2, PARP-1, Bax (Cell Signaling Technology; Beverly, MA), actin (Sigma-Aldrich), and anti-

MOL #79699

rabbit-horseradish peroxidase secondary antibodies (Promega) were used according to the instructions of the manufacturer.

Detection of ligand-induced macromolecular complex formation with LPA₂

LPA₂ forms a ternary complex with TRIP6 and NHERF2 (E et al., 2009; Lin et al., 2007; Xu et al., 2004). This complex is assembled via multiple protein-protein interactions that include: binding of NHERF2 to the C-terminal PSD95/Dlg/ZO-1 domain (PDZ)-binding motif of LPA₂, the binding of TRIP6 to the Zinc-finger-like CxxC motif of LPA₂, and binding of NHERF2 to the PDZ-binding motif of TRIP6 (E et al., 2009). To examine ligand-induced macromolecular complex formation, HEK293T cells were transfected with FLAG-LPA₂ and enhanced green fluorescent protein (EGFP)-NHERF2, and the cells were exposed to 10 μM GRI977143 for 10 min as described in detail in our previous publication (E et al., 2009). The complex was pulled down using anti-FLAG M2 monoclonal antibody-conjugated agarose beads (Sigma-Aldrich) and processed for western blotting using anti-EGFP (gift from Dr. A.P. Naren; UTHSC, TN), anti-FLAG (Sigma-Aldrich), and anti-TRIP6 (Bethyl Laboratories; Montgomery, TX) antibodies.

Statistical analysis

Data are expressed as mean ± SD or SEM for samples run in triplicates. Each experiment was repeated at least two times. Student's *t*-test was used for comparison between the control and treatment groups. A *p* value ≤0.05 was considered significant.

MOL #79699

RESULTS

Rational discovery of LPA₂ agonists

In a virtual screen using a structure-based pharmacophore of LPA₁ (Perygin, 2010), we serendipitously identified compound NSC12404, which was a weak agonist of LPA₂ (**Table 1 and Fig. 1**). Although this hit was not the intended target of that study, here we returned to this scaffold for the initiation of a virtual homology screen for other nonlipid ligands of LPA₂. With the use of this hit, we undertook a database search in the UC-DCC chemical library. The similarity search included the requirement for a fused tricyclic or bicyclic ring system and the presence of an acid moiety linked with a hydrocarbon chain. The similarity fingerprint metrics included: 1) extended connectivity fingerprint counts over 6 atoms, 2) functional class connectivity fingerprint counts over 4 atoms, and 3) functional class connectivity fingerprint counts over 6 atoms.

Similarity searches were performed separately using each similarity fingerprint to quantitate similarity. Hits meeting the 80% similarity threshold from each search were ranked based on the Tanimoto coefficient measure of similarity to the target molecule NSC12404 and the top 75 unique hits from each fingerprint search were selected for further analysis. The 225 compounds selected for further analysis were clustered based on Tanimoto coefficients calculated using Molecular ACCess System-key fingerprints (MACCS keys) and evaluated using the diversity subset function implemented in MOE. This selected a diverse subset of 27 compounds for biological evaluation by choosing the middle compounds in each cluster. These 27 compounds were tested in Ca²⁺ mobilization assays at a concentration of 10 μM using stable cell

MOL #79699

lines individually expressing LPA₂ and also in vector-transfected control cells (**Fig. 1 & Table 1**). Hits activating LPA₂ were further tested using cells expressing the other established and putative LPA GPCRs. Experimental testing of the selected compounds identified three new selective LPA₂ agonists: GRI977143, H2L5547924, and H2L5828102 (**Table 1**). NSC12404, H2L5547924, H2L5828102, and GRI977143 only activated LPA₂ and failed to activate any of the other established and putative LPA GPCRs when applied up to 10 μ M. A 10 μ M concentration of these compounds have also been tested for the inhibition of the Ca²⁺ response elicited by the \sim EC₇₅ concentration of LPA 18:1 at those receptors that the compound failed to activate when applied at 10 μ M. We found that at this high concentration NSC12404 and GRI977143 inhibited LPA₃ but none of the other receptors we tested were either activated or inhibited by these two compounds. H2L5547924 activated LPA₂ but partially inhibited LPA₁, LPA₃, LPA₄, GPR87, and P2Y10. H2L5828102 although was a specific agonist of LPA₂ but fully inhibited LPA₃ and partially inhibited LPA₁, GPR87 and P2Y10 (**Table 1**). Based on its lower EC₅₀ concentration to activate the LPA₂ receptor compared to NSC12404 and because it only inhibited the LPA₃ receptor compared to the H2L compounds we selected GRI977143 for further characterization in cell-based assays.

The LPA₂ computational model docked with LPA 18:1 suggests 13 residues that comprise the ligand binding pocket (**Fig. 2B-D and Table 2**). Computational docking of the four hits listed in **Table 1** indicates that these LPA₂ ligands interact with some additional residues unique to a specific agonist in addition to the 13 common residues (**Table 2 and Fig. 2B-D**). The model of GRI977143 docked to the LPA₂ structure is shown in **Fig. 2**. The docked structure shows that GRI977143 docks in the vicinity of

MOL #79699

the key residues R3.28, Q3.29, K7.36, and W4.64, which, we have previously shown are required for ligand activation of LPA₂ (Valentine et al., 2008). In addition, the model predicted an interaction with W5.40 that was unique to this ligand.

A structure-based pharmacophore was developed using the docking function of the MOE software (MOE, 2002). Compound NSC12404 and LPA were docked into a homology model of LPA₂ (Sardar et al., 2002; Valentine et al., 2008). In the pharmacophore model, we identified three feature sites based on the interactions between the agonists and the protein. We defined the key residues as those within 4.5 Å of our LPA₂ agonists. The pharmacophore features and the corresponding amino acid residues involved in ligand interactions are shown in **Fig. 2A**. This pharmacophore model has three features: a hydrophobic feature (green), a hydrogen bond acceptor (blue), and an anionic (red) feature. The four volume spheres in the pharmacophore with radii in the 2.8–4.2 Å range delineate the regions ideal for different types of chemical interactions with the ligand in the binding pocket. The distances between chemical features along with the radii of the four volume spheres are shown in **Fig. 2A**.

Effect of GRI977143 on cell growth

LPA can function as a mitogen or an antimitogen, depending on the cell type and the receptors it expresses (Tigyi et al., 1994). We tested GRI977143 for its effect on cell proliferation of vector- (**Fig. 3A**) and LPA₂-transduced MEF cells (**Fig. 3B**). LPA had no significant effect on the proliferation of empty vector-transduced MEF cells. Likewise, GRI977143 did not cause a significant increase in vector cell proliferation except at 72 hours ($p < 0.05$). In contrast, OTP significantly ($p < 0.001$) increased the growth of empty

MOL #79699

vector-transduced MEF cells from 24 hours onwards. The effects of LPA, OTP and GRI977143 on the growth of LPA₂-transduced MEF were all significant from 24 hours onwards.

Effect of GRI977143 on MM1 hepatoma cell invasion

The highly invasive rat hepatoma MM1 cells invade mesothelial cell monolayers in an LPA-dependent manner (Mukai and Akedo, 1999; Mukai et al., 2003; Uchiyama et al., 2007). LPA₂ receptor is abundantly expressed in MM1 cells (Gupte et al., 2011). Thus, we posed the question whether GRI977143-mediated activation of LPA₂ could stimulate the invasion of HUVEC monolayers by MM1 cells. Our results showed that whereas 1 μ M LPA already caused a significant increase in MM1 cell invasion, a higher 10 μ M concentration of GRI977143 was required to elicit the same significant increase in invasion (**Fig. 4**).

Effect of GRI977143 on LPA₂-mediated protection against Adriamycin-induced apoptosis

We examined the antiapoptotic properties of GRI977143 using Adriamycin to induce apoptosis. GRI977143 (10 μ M) decreased caspase 9 activation in LPA₂-transduced MEF cells by $46 \pm 4\%$; this decrease was similar in its magnitude to that of 1 μ M LPA, whereas 1 μ M OTP resulted in a slightly smaller $38 \pm 1\%$ decrease (**Fig. 5A**). GRI977143 did not affect caspase 9 activation in the vector-transduced cells, whereas LPA and OTP even in a 1 μ M concentration reduced caspase 9 activation by 20-24% (**Fig. 5A**). To guide our dosing considerations in the apoptosis assays, we also tested

MOL #79699

the dose-response relationship of our test compounds on Adriamycin-induced caspase 3 and 7 activation in vector- and LPA₂-transduced MEF cells. In the LPA₂-transduced MEF cells GRI977143 elicited a dose-dependent and significant protection above 3 μ M ($p < 0.01$, Supplemental figure 1). LPA and OTP dose-dependently protected LPA₂-transduced MEF cells starting from a concentration as low as 30 nM; however, at the highest 10 μ M concentration tested, LPA also had an inhibitory effect in the vector-transduced cells (Supplemental figure 1A&B). In contrast, when applied at 10 μ M, GRI977143 and OTP did not attenuate caspase 3 or caspase 7 in the vector-transduced cells (Supplemental Figure 1A). When applied at 10 μ M concentration, GRI977143 reduced caspase 3 and 7 activation on LPA₂-transduced MEF cells by $51 \pm 3\%$ and was approximately as potent as 3 μ M LPA or OTP (Fig. **5B** and supplemental figure 1).

To further characterize the effect of GRI977143 on apoptosis we measured Adriamycin-induced DNA fragmentation in vector- and LPA₂-transduced MEF cells. In LPA₂-transduced MEF cells GRI977143 reduced DNA fragmentation by $41 \pm 2\%$ ($p < 0.001$) compared to a modest $7 \pm 1\%$ protection in the vector-transduced cells ($p < 0.05$). 3 μ M LPA and 3 μ M OTP also protected LPA₂-transduced MEF cells by decreasing DNA fragmentation by $35 \pm 4\%$ and $32 \pm 1\%$, respectively (Fig. **5C**).

We also examined the effect of GRI977143 on caspase 8 activation in the Adriamycin-induced apoptosis model. Administration of 10 μ M GRI977143 resulted in a $41 \pm 5\%$ decrease in caspase 8 activation in LPA₂-transduced MEF cells. Treatments with 1 μ M LPA or 1 μ M OTP decreased caspase 8 activation by $36 \pm 1\%$ and $33 \pm 2\%$, respectively. A similar but lesser effect of LPA and OTP was noted in the vector-

MOL #79699

transduced cells, amounting to $12 \pm 2\%$ and $15 \pm 5\%$ decreases, respectively (**Fig. 5D**). These findings together establish that selective activation of LPA₂ receptor signaling by GRI977143 protects against Adriamycin-induced apoptosis by inhibiting caspase 3, 7, 8 and 9, and reducing DNA fragmentation.

GRI977143 reduces apoptosis induced by serum withdrawal in MEF cells

We also examined whether GRI977143 could provide the necessary trophic support to serum starved MEF cells expressing or lacking LPA₂ receptors. Experiments with this paradigm showed that 10 μ M GRI977143 was highly effective in reducing caspase 3, 7, 8, and 9 activation and also attenuated DNA fragmentation (**Fig. 6**). GRI977143 failed to cause any reduction in these apoptotic indicators in vector-transduced MEF cells. In contrast, LPA and OTP protected the vector-transduced MEF cells too. These results mirrored our findings in the Adriamycin-induced apoptosis paradigm, extending the role of LPA₂ activation to the prevention of serum withdrawal-induced apoptosis.

GRI977143 inhibits TNF α -induced apoptosis in IEC-6 intestinal epithelial cells

We showed earlier that LPA and OTP protects and rescues non-transformed IEC-6 crypt-like intestinal epithelial cells from TNF α -induced apoptosis (Deng et al., 2002; Deng et al., 2004; Deng et al., 2007; Deng et al., 2003). IEC-6 cells endogenously express LPA_{1/2/3/4} GPCRs, GPR87 and P2Y5 (Valentine et al., 2010). Thus, we tested the effect of GRI977143 in this model of extrinsic apoptosis. Treatment with TNF- α /CHX increased DNA fragmentation over 20-fold; the fragmentation was completely blocked by 10 μ M OTP and significantly reduced by 1 μ M LPA or 10 μ M GRI977143

MOL #79699

treatment (**Fig. 7**). Neither LPAR agonist caused any detectable change in DNA fragmentation when added to the cultures in the absence of TNF- α /CHX. These results extend our previous observations obtained in the Adriamycin-induced intrinsic apoptosis model to the TNF- α -induced model mediated via the extrinsic apoptosis pathway.

Effect of GRI977143 on Bax translocation and PARP-1 cleavage induced by Adriamycin or serum withdrawal

Because GRI977143 reduced activation of caspases 3, 7, 8, and 9, we tested the effect of 10 μ M GRI977143 on Bax translocation to the mitochondria induced by Adriamycin or serum withdrawal. As shown in **Fig. 8A**, 10 μ M GRI977143 treatment maintained a high level of Bax in the cytoplasm of LPA₂-transduced MEF cells after Adriamycin treatment, consequently reducing its translocation to the mitochondria. GRI977143 failed to reduce Bax translocation in the vector-transduced MEFs. In the serum withdrawal model of apoptosis we did not detect any change in the cytosolic Bax level (**Fig. 8B**).

GRI977143 treatment (10 μ M) also reduced PARP-1 cleavage after both apoptosis-inducing treatments (**Fig. 8C-D**). This effect was not observed in the vector-transduced cells. These experiments are consistent with the hypothesis that GRI977143 attenuates the activation of the mitochondrial apoptosis pathway through a mechanism that requires the LPA₂ receptor.

Effect of GRI977143 on ERK1/2 activation

MOL #79699

To elucidate some of the molecular mechanisms responsible for the antiapoptotic effect of GRI977143 we investigated its effect on the activation of ERK1/2 kinases, which is a required step in LPA₂ receptor-mediated antiapoptotic signaling (Deng et al., 2002; Deng et al., 2003; E et al., 2009). Treatment with 10 μM GRI977143 for 10 min increased ERK1/2 activation 9.6-fold in LPA₂-transduced MEF cells but did not alter the basal activity of these kinases in the vector-transduced cells (**Fig. 9A-B**). This result supports the hypothesis that the prosurvival effect of GRI977143 detected in different intrinsic and extrinsic apoptosis models is mediated by the LPA₂ receptor and involves ERK1/2 activation.

Effect of GRI977143 on the assembly of a macromolecular complex between LPA₂ TRIP6 and NHERF2

LPA₂ receptor-mediated supramolecular complex formation is required for the protection against Adriamycin-induced apoptosis (E et al., 2009). To further elucidate molecular mechanisms activated by GRI977143, we investigated its effect on agonist-induced signalosome assembly between TRIP6, NHERF2 and the C-terminus of LPA₂. This macromolecular complex plays an important role in the antiapoptotic effect via stimulation of the ERK1/2 and protein kinase B- nuclear factor κB (Akt-NFκB) survival pathways. GRI977143 elicited the assembly of the macromolecular complex indicated by the recruitment of TRIP6 and EGFP-NHERF2 to the LPA₂ receptor (**Fig. 9C**). Only trace amounts of the ternary complex were detected in the vehicle-treated cell lysates, indicating that activation of LPA₂ by GRI977143 elicited the assembly of the signaling complex.

MOL #79699

DISCUSSION

LPA's growth factor-like actions and its simple chemical structure make it an ideal candidate for drug discovery. A major obstacle in developing LPA analogs is their high degree of hydrophobicity that makes these agents nonideal drug candidates. Another complicating factor is the multiplicity of LPA GPCRs, which represents a significant challenge to the development of compounds specific to a single target such as LPA₂. Our group has been developing and validating computational models of the putative ligand binding pockets of LPA GPCRs (Fujiwara et al., 2007; Fujiwara et al., 2005; Parrill et al., 2000; Valentine et al., 2008; Wang et al., 2001). Our previous work aimed at the virtual discovery of LPA₁-specific compounds has serendipitously identified NSC12404, which is a weak but specific agonist of LPA₂ (Perygin, 2010). In the present study, we used this hit for virtual screening of the GRI and H2L chemical libraries. This approach identified three new selective nonlipid LPA₂ agonists: GRI977143, H2L5547924, and H2L5828102 (**Table 1**).

We selected GRI977143 for initial characterization in cell-based assays and compared its pharmacological and signaling properties with those of LPA and the previously identified LPA mimic OTP. The other compounds, NSC12404, H2L5547924, and H2L5828102 might be worthy of detailed characterization and synthetic improvements in the future. GRI977143 was a specific agonist of only LPA₂ when tested for agonist or antagonist activity at up to 10 μ M concentration at five established and two putative LPA GPCRs. It is noteworthy that this compound above 10 μ M also showed a modest partial inhibition of LPA₃. One of our strategies utilized MEF cells derived from LPA_{1&2} DKO

MOL #79699

mice (Lin et al., 2007). The parental MEF cells do not express functional LPA_{1/2/3} receptors but express LPA_{4/5/6} transcripts. Thus, these MEF cells can be considered an LPA receptor null host cell line for LPA_{1/2/3}, which belong to the endothelial differentiation gene (EDG) family LPA receptors. Knock in of LPA₂ rendered these MEF cells responsive to LPA with pharmacological properties similar to those of LPA₂ established in other cell types endogenously expressing this receptor subtype (E et al., 2009; Lin et al., 2007). The modest but sometimes significant antiapoptotic responses that were elicited in the vector-transduced MEF cells in response to LPA and OTP are likely due to activation by LPA_{4/5/6} receptors. GRI977143 had no effect in the vector-transduced MEF cells with the exception of a minimal reduction in DNA fragmentation in the Adriamycin model of apoptosis (**Fig. 5C**). There was no such detectable effect of GRI977143 in the serum withdrawal-induced apoptosis model (**Fig. 6C**). We do not know the reason for the effect of GRI977143 on DNA fragmentation in the control MEF cells in the Adriamycin model only, but it might be due to some yet unknown off-target effect of the compound. Certainly, the lack of effect of GRI977143 in vector-transduced MEF cells on Ca²⁺ mobilization (data not shown), on caspases 3, 7, 8, and 9, on DNA fragmentation, and on ERK1/2 activation are all consistent with the hypothesis that specific activation of LPA₂ is responsible for these same responses that we consistently detected in the MEF cells expressing the LPA₂ receptor. It is also important to recognize that GRI977143 protected IEC-6 cells from apoptosis, which endogenously express multiple LPA GPCR subtypes. This result is the first evidence that we know of in the literature that specific activation of LPA₂ is sufficient to evoke an antiapoptotic effect and this effect is not limited to the LPA₂ knock-in MEF cells.

MOL #79699

We also showed that specific stimulation of the LPA₂ receptor subtype promotes cell growth (**Fig. 3**). This is the first pharmacological evidence that this receptor subtype mediates mitogenesis. Surprisingly, the LPA receptor antagonist OTP and GRI977143 had equally robust activity on cell proliferation. We note that OTP and GRI977143 after 3 days also promoted the growth of vector-transduced MEF cells, which might be due to off-target or indirect effects. We cannot exclude the possibility that OTP and GRI977143 somehow potentiated the effect of the 1.5% serum present in the medium. There might be differences in the pharmacokinetic properties of these ligands, which could explain the differences we noted. Future experiments will have to address the differences on cell growth observed between these ligands.

LPA has been shown to promote cancer cell invasion and metastasis. We tested the effect of GRI977143 in an in vitro invasion model that has been considered a realistic model of metastasis (Mukai et al., 2005; Mukai et al., 2000; Uchiyama et al., 2007). Stimulation of MM1 hepatocarcinoma cells with GRI977143 elicited a dose-dependent increase in the number of cells that penetrated the HUVEC monolayer (**Fig. 4**). However, this effect, although significant at a 10 μM concentration of GRI977143, was modest compared to that of LPA. The MM1 cells express LPA₂ >> LPA₁ > LPA₆ > LPA₅ > LPA₄ transcripts, whereas HUVECs express LPA₅ >> LPA₄ > GPR87 ~ LPA₁ > LPA₂ transcripts determined by quantitative RT-PCR (Lee & Tigyi – unpublished). The increase in GRI977143-induced invasion of MM1 cells is likely to represent the effect of selective stimulation of LPA₂ in the invading MM1 cells rather than in HUVEC due to the very low expression of this receptor subtype in the cells of the monolayer (Gupte et al.,

MOL #79699

2011). Thus, our present results provide new pharmacological evidence that activation of LPA₂ can promote invasion and metastasis.

Studies have already established the role of the LPA₂ receptor in protecting cells from programmed cell death (Deng et al., 2002; E et al., 2009; Lin et al., 2007; Sun et al., 2010; Taghavi et al., 2008; Yu et al., 2008). The LPA₂-specific agonist properties of GRI977143 allowed us to test this hypothesis in the LPA₂ knock-in MEF cells and in IEC-6 cells, the latter of which endogenously expresses multiple LPA GPCRs (Deng et al., 2002; Deng et al., 2004; Deng et al., 2007; Deng et al., 2003). GRI977143 reduced the activation of the executioner caspases 3 and 7 and its upstream regulator caspases 8 and 9. Attenuation of these caspases explains the reduction of PARP-1 cleavage and DNA fragmentation we observed. These mechanisms were common to GRI977143 regardless of whether apoptosis was elicited via the extrinsic pathway or the intrinsic pathway (**Figs. 5, 6, 7**). Both LPA and OTP activate these same mechanisms but also activate multiple LPA GPCRs (Deng et al., 2002; Deng et al., 2004; Deng et al., 2007; Deng et al., 2003). Thus, we propose that specific activation of LPA₂ is sufficient to protect cells from apoptosis. The specific agonist properties of GRI977143 might represent an advantage over LPA and other receptor-nonspecific LPA mimics that also stimulate LPA₁ receptor subtype activation, which has been shown to promote cell death via anoikis in tumor cells (Furui et al., 1999), in cardiac myocytes (Chen et al., 2006), and in pulmonary epithelial cells (Funke et al., 2012).

LPA₂-mediated activation of the ERK1/2 prosurvival kinases is a required event in antiapoptotic signaling (Deng et al., 2004; E et al., 2009; Lin et al., 2007). Consistent

MOL #79699

with our previous results obtained with LPA and OTP (Deng et al., 2007; E et al., 2009; Lin et al., 2007), GRI977143 treatment resulted in a robust ERK1/2 activation. We have previously shown that in addition to the Gi protein-mediated signals demonstrated by the partial pertussis toxin-sensitivity of the effect (Deng et al., 2002; Deng et al., 2004), the LPA₂-mediated antiapoptotic effect requires additional ligand-induced assembly of a C-terminal macromolecular complex consisting of LPA₂, TRIP6, and a homodimer of NHERF2 (E et al., 2009; Lai et al., 2005; Lin et al., 2007). Activation of LPA₂ regulates the c-Src-mediated phosphorylation of TRIP6 at the Tyr-55 and Pro-58 residue, which in turn promotes LPA-induced ERK1/2 activation (Lai et al., 2005). We found that GRI977143 elicited the assembly of this signalosome (**Fig. 9C**), which can explain the concomitant robust ERK1/2 activation (**Fig. 9A-B**).

Taken altogether, the present findings indicate that nonlipid LPA₂-specific agonists, such as those described here, represent an excellent starting point for the development of lead compounds with potential therapeutic utility for the prevention of programmed cell death involved in many types of degenerative and inflammatory diseases.

MOL #79699

ACKNOWLEDGMENTS

The authors thank Drs. Jerold Chun (Scripps Institute) for providing the LPA₁ and LPA₂ mice, Fumikazu Okajima, Takao Shimizu, Norihisa Fujita, and Michiko Mukai for providing the different cell types used in the study, A.P. Naren for providing the anti-EGFP antibody and William Seibel (University of Cincinnati) for his assistance with the similarity search of the UC-DCC library. The MOE program was donated by the Chemical Computing Group and is greatly appreciated.

MOL #79699

AUTHORSHIP CONTRIBUTIONS

Participated in research design: Kiss, Fells, Gupte, Lee, Liu, Nusser, Ray, Lin, Parrill, Sümegi, Miller, Tigyi

Conducted experiments: Kiss, Fells, Gupte, Lee, Liu, Nusser, Lim, Ray, Lin, Parrill, Tigyi

Contributed new reagents or analytic tools: N/A

Performed data analysis: Kiss, Fells, Gupte, Lee, Liu, Nusser, Lim, Ray, Lin, Parrill, Miller, Tigyi

Wrote or contributed to the writing of the manuscript: Kiss, Fells, Lee, Nusser, Lim, Ray, Lin, Parrill, Tigyi

MOL #79699

REFERENCES

- Ballesteros JAW, H (1995) Integrated Methods for the Construction of Three Dimensional Models and Computational Probing of Structure-Function Relations in G-Protein Coupled Receptors. *Methods Neurosci* **25**:366-425.
- Brinkmann V, Billich A, Baumruker T, Heining P, Schmouder R, Francis G, Aradhye S and Burtin P (2010) Fingolimod (FTY720): discovery and development of an oral drug to treat multiple sclerosis. . *Nat Rev Drug Discov* **2** 9:883-897.
- Chen J, Han Y, Zhu W, Ma R, Han B, Cong X, Hu S and Chen X (2006) Specific receptor subtype mediation of LPA-induced dual effects in cardiac fibroblasts. *FEBS letters* **580**(19):4737-4745.
- Deng W, Balazs L, Wang DA, Van Middlesworth L, Tigyi G and Johnson LR (2002) Lysophosphatidic acid protects and rescues intestinal epithelial cells from radiation- and chemotherapy-induced apoptosis. *Gastroenterology* **123**(1):206-216.
- Deng W, Poppleton H, Yasuda S, Makarova N, Shinozuka Y, Wang DA, Johnson LR, Patel TB and Tigyi G (2004) Optimal lysophosphatidic acid-induced DNA synthesis and cell migration but not survival require intact autophosphorylation sites of the epidermal growth factor receptor. *J Biol Chem* **279**(46):47871-47880.
- Deng W, Shuyu E, Tsukahara R, Valentine WJ, Durgam G, Gududuru V, Balazs L, Manickam V, Arsura M, VanMiddlesworth L, Johnson LR, Parrill AL, Miller DD and Tigyi G (2007) The lysophosphatidic acid type 2 receptor is required for protection against radiation-induced intestinal injury. *Gastroenterology* **132**(5):1834-1851.

MOL #79699

Deng W, Wang DA, Gosmanova E, Johnson LR and Tigyi G (2003) LPA protects intestinal epithelial cells from apoptosis by inhibiting the mitochondrial pathway.

Am J Physiol Gastrointest Liver Physiol **284**(5):G821-829.

Durgam GG, Tsukahara R, Makarova N, Walker MD, Fujiwara Y, Pigg KR, Baker DL,

Sardar VM, Parrill AL, Tigyi G and Miller DD (2006) Synthesis and pharmacological evaluation of second-generation phosphatidic acid derivatives

as lysophosphatidic acid receptor ligands. *Bioorg Med Chem Lett* **16**(3):633-640.

E S, Lai YJ, Tsukahara R, Chen CS, Fujiwara Y, Yue J, Yu JH, Guo H, Kihara A, Tigyi

G and Lin FT (2009) The LPA2 receptor-mediated supramolecular complex formation regulates its antiapoptotic effect. *J Biol Chem*.

Fischer DJ, Nusser N, Virag T, Yokoyama K, Wang D, Baker DL, Bautista D, Parrill AL

and Tigyi G (2001) Short-chain phosphatidates are subtype-selective antagonists of lysophosphatidic acid receptors. *Mol Pharmacol* **60**(4):776-784.

Fujiwara Y, Osborne DA, Walker MD, Wang DA, Bautista DA, Liliom K, Van Brocklyn

JR, Parrill AL and Tigyi G (2007) Identification of the hydrophobic ligand binding pocket of the S1P1 receptor. *J Biol Chem* **282**(4):2374-2385.

Fujiwara Y, Sardar V, Tokumura A, Baker D, Murakami-Murofushi K, Parrill A and Tigyi

G (2005) Identification of residues responsible for ligand recognition and regioisomeric selectivity of lysophosphatidic acid receptors expressed in mammalian cells. *J Biol Chem* **280**(41):35038-35050.

Funke M, Zhao Z, Xu Y, Chun J and Tager AM (2012) The lysophosphatidic acid

receptor LPA1 promotes epithelial cell apoptosis after lung injury. *Am J Respir Cell Mol Biol* **46**(3):355-364.

MOL #79699

- Furui T, LaPushin R, Mao M, Khan H, Watt SR, Watt MA, Lu Y, Fang X, Tsutsui S, Siddik ZH, Bast RC and Mills GB (1999) Overexpression of edg-2/vzg-1 induces apoptosis and anoikis in ovarian cancer cells in a lysophosphatidic acid-independent manner. *Clin Cancer Res* **5**(12):4308-4318.
- Gupte R, Patil R, Liu J, Wang Y, Lee SC, Fujiwara Y, Fells J, Bolen AL, Emmons-Thompson K, Yates CR, Siddam A, Panupinthu N, Pham TC, Baker DL, Parrill AL, Mills GB, Tigyi G and Miller DD (2011) Benzyl and Naphthalene Methylphosphonic Acid Inhibitors of Autotaxin with Anti-invasive and Anti-metastatic Activity. *ChemMedChem* **6**(5):922-935.
- Hanson MA, Roth CB, Jo E, Griffith MT, Scott FL, Reinhart G, Desale H, Clemons B, Cahalan SM, Schuerer SC, Sanna MG, Han GW, Kuhn P, Rosen H and Stevens RC (2012) Crystal structure of a lipid G protein-coupled receptor. *Science* **335**(6070):851-855.
- Lai YJ, Chen CS, Lin WC and Lin FT (2005) c-Src-mediated phosphorylation of TRIP6 regulates its function in lysophosphatidic acid-induced cell migration. *Mol Cell Biol* **25**(14):5859-5868.
- Lai YJ, Lin WC and Lin FT (2007) PTPL1/FAP-1 negatively regulates TRIP6 function in lysophosphatidic acid-induced cell migration. *The Journal of biological chemistry* **282**(33):24381-24387.
- Li C, Dandridge KS, Di A, Marrs KL, Harris EL, Roy K, Jackson JS, Makarova NV, Fujiwara Y, Farrar PL, Nelson DJ, Tigyi GJ and Naren AP (2005) Lysophosphatidic acid inhibits cholera toxin-induced secretory diarrhea through CFTR-dependent protein interactions. *J Exp Med* **202**(7):975-986.

MOL #79699

Lin FT, Lai YJ, Makarova N, Tigyi G and Lin WC (2007) The lysophosphatidic acid 2 receptor mediates down-regulation of Siva-1 to promote cell survival. *J Biol Chem* **282**(52):37759-37769.

Lipinski CA (2003) Chris Lipinski discusses life and chemistry after the Rule of Five. *Drug Discov Today* **8**(1):12-16.

MOE (2002), Chemical Computing Group, Montreal.

Mukai M and Akedo H (1999) [Induction of tumor invasion by lysophosphatidic acid and inhibition of tumor invasion by cyclic phosphatidic acid]. *Tanpakushitsu Kakusan Koso* **44**(8 Suppl):1126-1131.

Mukai M, Iwasaki T, Tatsuta M, Togawa A, Nakamura H, Murakami-Murofushi K, Kobayashi S, Imamura F and Inoue M (2003) Cyclic phosphatidic acid inhibits RhoA-mediated autophosphorylation of FAK at Tyr-397 and subsequent tumor-cell invasion. *Int J Oncol* **22**(6):1247-1256.

Mukai M, Kusama T, Hamanaka Y, Koga T, Endo H, Tatsuta M and Inoue M (2005) Cross talk between apoptosis and invasion signaling in cancer cells through caspase-3 activation. *Cancer Res* **65**(20):9121-9125.

Mukai M, Nakamura H, Tatsuta M, Iwasaki T, Togawa A, Imamura F and Akedo H (2000) Hepatoma cell migration through a mesothelial cell monolayer is inhibited by cyclic AMP-elevating agents via a Rho-dependent pathway. *FEBS Lett* **484**(2):69-73.

Murakami M, Shiraishi A, Tabata K and Fujita N (2008) Identification of the orphan GPCR, P2Y(10) receptor as the sphingosine-1-phosphate and lysophosphatidic acid receptor. *Biochem Biophys Res Commun* **371**(4):707-712.

MOL #79699

Ohta H, Sato K, Murata N, Damirin A, Malchinkhuu E, Kon J, Kimura T, Tobo M, Yamazaki Y, Watanabe T, Yagi M, Sato M, Suzuki R, Murooka H, Sakai T, Nishitoba T, Im DS, Nochi H, Tamoto K, Tomura H and Okajima F (2003) Ki16425, a subtype-selective antagonist for EDG-family lysophosphatidic acid receptors. *Mol Pharmacol* **64**(4):994-1005.

Parrill AL, Wang D, Bautista DL, Van Brocklyn JR, Lorincz Z, Fischer DJ, Baker DL, Liliom K, Spiegel S and Tigyi G (2000) Identification of Edg1 receptor residues that recognize sphingosine 1-phosphate. *J Biol Chem* **275**(50):39379-39384.

Perygin DH (2010) Identification of Non-Lipid LPA Receptor Agonists and Antagonists Through In Silico Screening, in *Chemistry* p 130, University of Memphis, Memphis.

Ray RM, Bhattacharya S and Johnson LR (2011) Mdm2 inhibition induces apoptosis in p53 deficient human colon cancer cells by activating p73- and E2F1-mediated expression of PUMA and Siva-1. *Apoptosis* **16**(1):35-44.

Sardar VM, Bautista DL, Fischer DJ, Yokoyama K, Nusser N, Virag T, Wang DA, Baker DL, Tigyi G and Parrill AL (2002) Molecular basis for lysophosphatidic acid receptor antagonist selectivity. *Biochim Biophys Acta* **1582**(1-3):309-317.

Sun Y, Nam JS, Han DH, Kim NH, Choi HK, Lee JK, Rhee HJ and Huh SO (2010) Lysophosphatidic acid induces upregulation of Mcl-1 and protects apoptosis in a PTX-dependent manner in H19-7 cells. *Cell Signal* **22**(3):484-494.

Swaney JS, Chapman C, Correa LD, Stebbins KJ, Broadhead AR, Bain G, Santini AM, Darlington J, King CD, Baccei CS, Lee C, Parr TA, Roppe JR, Seiders TJ, Ziff J, Prasit P, Hutchinson JH, Evans JF and Lorrain DS (2011) Pharmacokinetic and

MOL #79699

- pharmacodynamic characterization of an oral lysophosphatidic acid type 1 receptor-selective antagonist. *J Pharmacol Exp Ther* **336**(3):693-700.
- Tabata K, Baba K, Shiraishi A, Ito M and Fujita N (2007) The orphan GPCR GPR87 was deorphanized and shown to be a lysophosphatidic acid receptor. *Biochem Biophys Res Commun* **363**(3):861-866.
- Taghavi P, Verhoeven E, Jacobs JJ, Lambooi JP, Stortelers C, Tanger E, Moolenaar WH and van Lohuizen M (2008) In vitro genetic screen identifies a cooperative role for LPA signaling and c-Myc in cell transformation. *Oncogene* **27**(54):6806-6816.
- Tigyi G (2010) Aiming drug discovery at lysophosphatidic acid targets. *Br J Pharmacol* **161**(2):241-270.
- Trott O and Olson AJ (2010) AutoDock Vina: improving the speed and accuracy of docking with a new scoring function, efficient optimization, and multithreading. *J Comput Chem* **31**(2):455-461.
- Uchiyama A, Mukai M, Fujiwara Y, Kobayashi S, Kawai N, Murofushi H, Inoue M, Enoki S, Tanaka Y, Niki T, Kobayashi T, Tigyi G and Murakami-Murofushi K (2007) Inhibition of transcellular tumor cell migration and metastasis by novel carba-derivatives of cyclic phosphatidic acid. *Biochim Biophys Acta* **1771**(1):103-112.
- Valentine WJ, Fells JI, Perygin DH, Mujahid S, Yokoyama K, Fujiwara Y, Tsukahara R, Van Brocklyn JR, Parrill AL and Tigyi G (2008) Subtype-specific residues involved in ligand activation of the endothelial differentiation gene family lysophosphatidic acid receptors. *J Biol Chem* **283**(18):12175-12187.

MOL #79699

Valentine WJ, Kiss GN, Liu J, E S, Gotoh M, Murakami-Murofushi K, Pham TC, Baker DL, Parrill AL, Lu X, Sun C, Bittman R, Pyne NJ and Tigyi G (2010) (S)-FTY720-vinylphosphonate, an analogue of the immunosuppressive agent FTY720, is a pan-antagonist of sphingosine 1-phosphate GPCR signaling and inhibits autotaxin activity. *Cell Signal* **22**(10):1543-1553.

Wang DA, Lorincz Z, Bautista DL, Liliom K, Tigyi G and Parrill AL (2001) A single amino acid determines lysophospholipid specificity of the S1P1 (EDG1) and LPA1 (EDG2) phospholipid growth factor receptors. *J Biol Chem* **276**(52):49213-49220.

Williams JR, Khandoga AL, Goyal P, Fells JI, Perygin DH, Siess W, Parrill AL, Tigyi G and Fujiwara Y (2009) Unique ligand selectivity of the GPR92/LPA5 lysophosphatidate receptor indicates role in human platelet activation. *J Biol Chem* **284**(25):17304-17319.

Xu J, Lai YJ, Lin WC and Lin FT (2004) TRIP6 enhances lysophosphatidic acid-induced cell migration by interacting with the lysophosphatidic acid 2 receptor. *The Journal of biological chemistry* **279**(11):10459-10468.

Yu S, Murph MM, Lu Y, Liu S, Hall HS, Liu J, Stephens C, Fang X and Mills GB (2008) Lysophosphatidic acid receptors determine tumorigenicity and aggressiveness of ovarian cancer cells. *J Natl Cancer Inst* **100**(22):1630-1642.

MOL #79699

FOOTNOTES

This research was supported by a grant from the National Institutes of Health, National Institute of Allergy Medical Countermeasures Radiological and Nuclear Threats Program [AI80405].

Financial disclosure: GT is a founder of RxBio, Inc.

MOL #79699

FIGURE LEGENDS

Figure 1. Receptor specificity of the prototype hit compound NSC12404 and in silico hit GRI977143 indicated by LPA GPCR-activated Ca^{2+} -transients in cell lines expressing the individual LPA GPCR subtypes. The curves shown in this figure are representative of at least two experiments.

Figure 2. Pharmacophore development for the LPA_2 GPCR. The three-dimensional pharmacophore generated (panel A) was based on the common structural features of docked LPA (panel B), GRI977143 (panel C), and NSC12404 (panel D). The pharmacophore properties are shown in red (anionic), blue (hydrogen bond acceptor), and green (hydrophobic interaction) in panel 1A. The volume of the binding site is shown in white spheres. The three agonists (ball and stick) used for pharmacophore development are shown with interactions with key amino acid residues (purple) within 4.5 Å of the previously validated ligand binding pocket.

Figure 3. Effects of LPA (1 μM), OTP (1 μM) and GRI977143 (10 μM) on fibroblast growth. Panel A shows the growth curves of the vector- and panel B of the LPA_2 -transduced MEF cells. Values are means \pm S.D and representative of two independent experiments (* $p \leq 0.05$, ** $p \leq 0.01$, *** $p \leq 0.001$).

Figure 4. Effect of GRI977143 on the invasion of HUVEC monolayers by MM1 hepatocarcinoma cells. Data are the means of 5 non-overlapping fields and representative of two independent experiments (* $p \leq 0.05$, *** $p \leq 0.001$).

MOL #79699

Figure 5. Effects of LPA and OTP (panels A, D: 1 μ M; panels B, C: 3 μ M), and GRI977143 (10 μ M) on Adriamycin-induced apoptotic signaling in vector- (open bars) or LPA₂-transduced (filled bars) MEF cells. Bars represent the mean of triplicate wells and the data are representative of three independent experiments. (* $p \leq 0.05$, ** $p \leq 0.01$, *** $p \leq 0.001$).

Figure 6. Effects of LPA (panels A, B: 3 μ M; panels C, D: 10 μ M), OTP (3 μ M) and GRI977143 (10 μ M) on serum withdrawal-induced apoptotic signaling in vector- (open bars) or LPA₂-transduced (filled bars) MEF cells. Bars represent the mean of triplicate wells and the data are representative of three independent experiments. (* $p \leq 0.05$, ** $p \leq 0.01$, *** $p \leq 0.001$).

Figure 7. Effects of LPA (1 μ M), OTP (10 μ M), and GRI977143 (10 μ M) on DNA-fragmentation elicited via extrinsic apoptosis induced by TNF α and CHX treatment in IEC-6 cells. Bars represent the mean of triplicate wells, and the data are representative of two experiments. (***) $p \leq 0.01$.

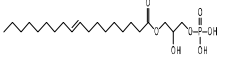
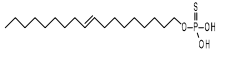
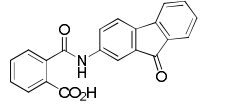
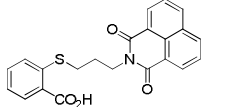
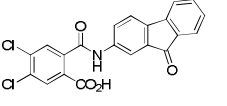
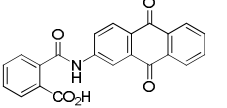
Figure 8. Effects of GRI977143 on cytoplasmic Bax levels and PARP-1 cleavage in vector- or LPA₂-transduced MEF cells following Adriamycin- or serum withdrawal-induced apoptosis. The western blots shown are representative of three experiments.

Figure 9. Signaling pathways activated by LPA (1 μ M), OTP (1 μ M), or GRI977143 (10 μ M). Representative western blots (panel A) and densitometry (panel B) of the mean ERK1/2 activation in vector- (open bars) and LPA₂-transduced (filled bars) MEF cells after GRI977143 treatment. Data were normalized for equal loading based on actin and

MOL #79699

are representative of three independent experiments ($^*p \leq 0.05$, $^{***}p \leq 0.001$). Panel C shows that GRI977143 elicits macromolecular complex assembly between FLAG-LPA₂, EGFP-NHERF2, and endogenous TRIP6. The blot shown is representative of two co-transfection experiments.

Table 1. LPA receptor activated Ca²⁺ mobilization profiles for hit compounds.

Compound	Structure	Log P	LPA ₁		LPA ₂		LPA ₃		LPA ₄		LPA ₅		GPR87		P2Y10	
			E _{max}	EC ₅₀	E _{max}	EC ₅₀	E _{max}	EC ₅₀								
LPA 18:1		6.12	E _{max} 100	EC ₅₀ 0.13	E _{max} 100	EC ₅₀ 0.03	E _{max} 100	EC ₅₀ 0.08	E _{max} 100	EC ₅₀ 0.25	E _{max} 100	EC ₅₀ 0.015	E _{max} 100	EC ₅₀ 0.049	E _{max} 100	EC ₅₀ 0.03
OTP		7.72	E _{max} 50	EC ₅₀ 0.65	E _{max} 80	EC ₅₀ 0.47	E _{max} 50	EC ₅₀ 0.30	E _{max} 70	EC ₅₀ 2.0	E _{max} 100	EC ₅₀ 0.003	E _{max} 40	EC ₅₀ 3.0	NE	NE
NSC 12404		3.25	NE	NE	E _{max} 82	EC ₅₀ 9.5	I _{max} 61	IC ₅₀ 8.5	NE	NE	NE	NE	NE	NE	NE	NE
GRI 977143		3.88	NE	NE	E _{max} 75	EC ₅₀ 3.3	I _{max} 100	IC ₅₀ 6.6	NE	NE	NE	NE	NE	NE	NE	NE
H2L 5547924		4.36	I _{max} 21	IC ₅₀ 1.90	E _{max} 34	EC ₅₀ 2.8	I _{max} 66	IC ₅₀ 3.5	I _{max} 51	IC ₅₀ 1.3	NE	NE	I _{max} 31	IC ₅₀ 0.88	I _{max} 34	IC ₅₀ 1.4
H2L 5828102		2.78	I _{max} 29	IC ₅₀ 0.20	E _{max} 37	EC ₅₀ 3.3	I _{max} 100	IC ₅₀ 1.9	NE	NE	NE	NE	I _{max} 21	IC ₅₀ 3.9	I _{max} 39	IC ₅₀ 1.1

Log P = Log partition coefficient, NE = no effect up to 10 μM of the ligand, the maximal concentration tested in the present experiments. Every compound was tested on every receptor subtype for agonist activity up to 10 μM and the E_{max} value listed in the table is normalized to the maximal response of LPA 18:1 at 10 μM. Those compounds that failed to activate a given receptor were tested for the inhibition of the LPA 18:1 response. I_{max} = % inhibition of the ~E_{max}75 LPA 18:1 response for a given receptor subtype using 10 μM of the antagonist. EC₅₀ and IC₅₀ concentrations are given in μM for dose-response curves covering the 30 nM - 10 μM range (see figure 1). For determination of IC₅₀ values, dose-response curves were generated using ~E_{max}75 concentration of LPA 18:1 for a given LPA receptor subtype and the ligand was coapplied in concentrations ranging from 30 nM to 10 μM.

MOL #79699

Table 2

	EC₅₀ (μM)	Common Residues to all agonists predicted to be within 4.5 Å of the docked ligand
LPA 18:1	0.014	R3.28, Q3.29, G3.30, L3.32, D3.33, L3.34, W4.64, L5.37, R5.38, W6.48, K7.36, F7.38, L7.39
		Unique residues to a specific ligand predicted to be within 4.5 Å of the docked ligand
OTP	0.09	W5.40, L6.55
NSC 12404	9.5	T2.64
GRI977143	3.3	W5.40
H2L 5547924	2.9	Interacts with all common residues but some interactions are less favorable than with LPA or OTP
H2L 5828102	16.7	L7.32, T2.64, S270

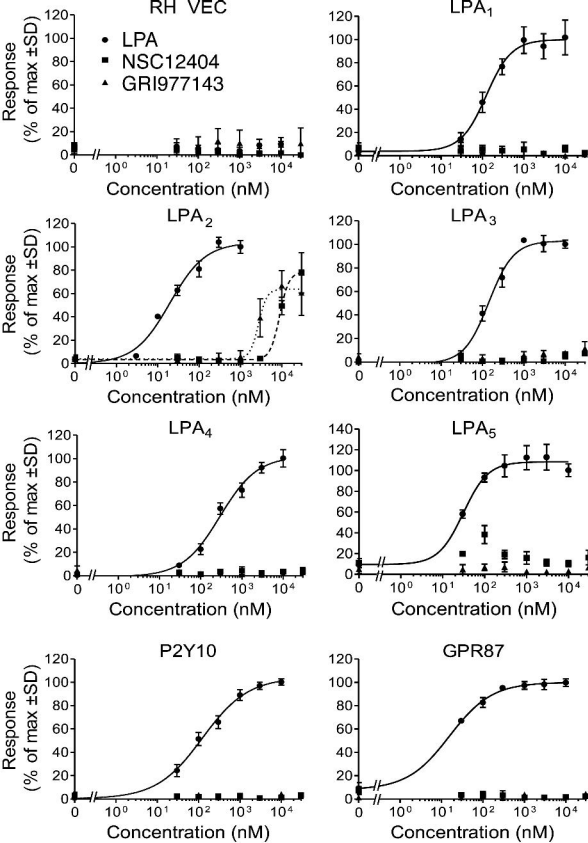


Figure 1

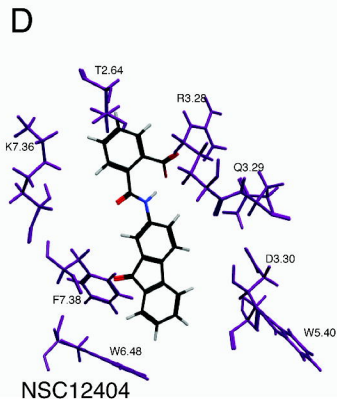
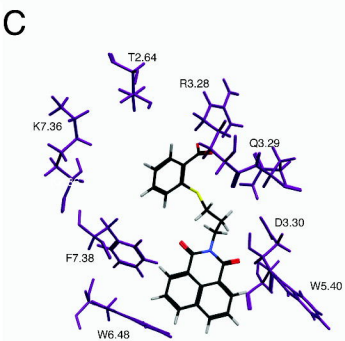
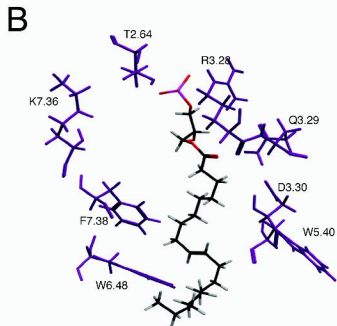
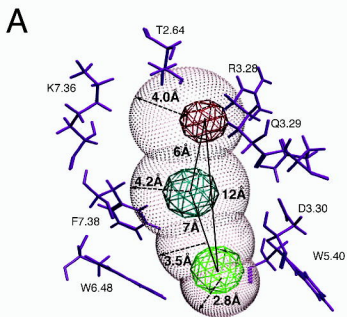


Figure 2

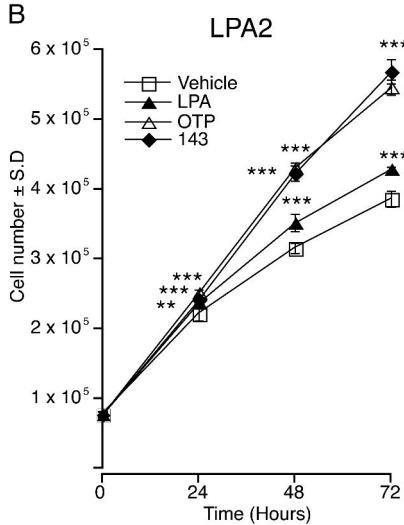
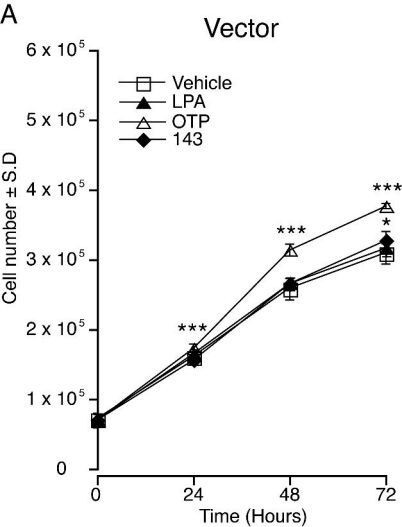


Figure 3

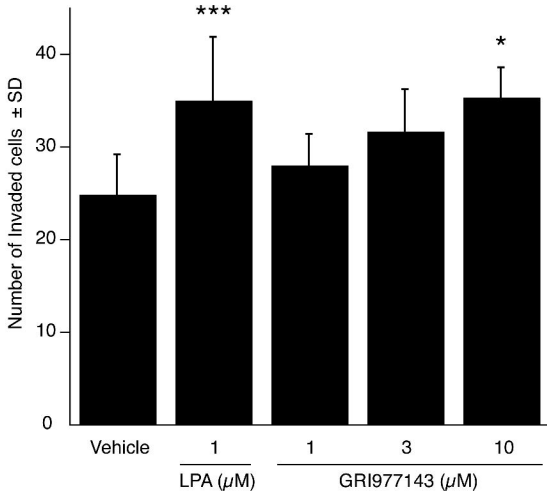


Figure 4

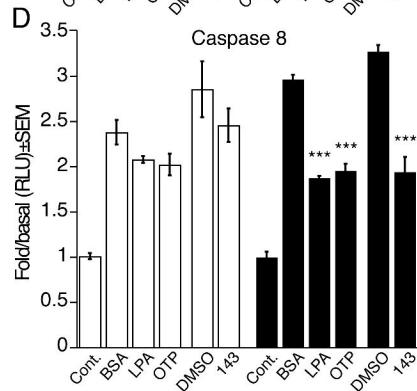
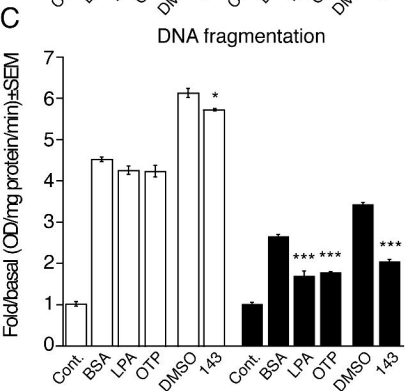
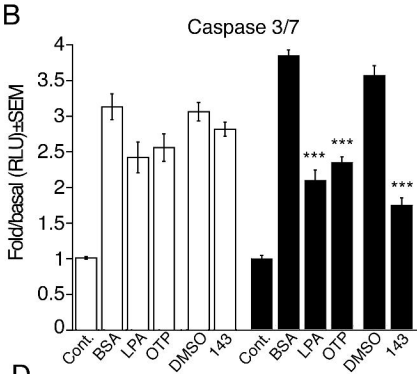
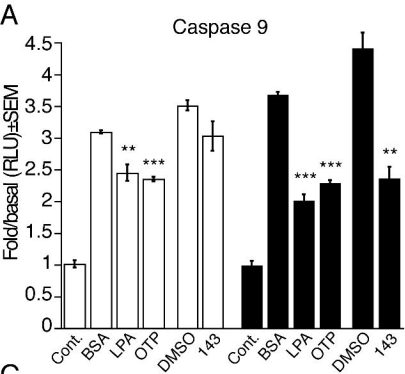


Figure 5

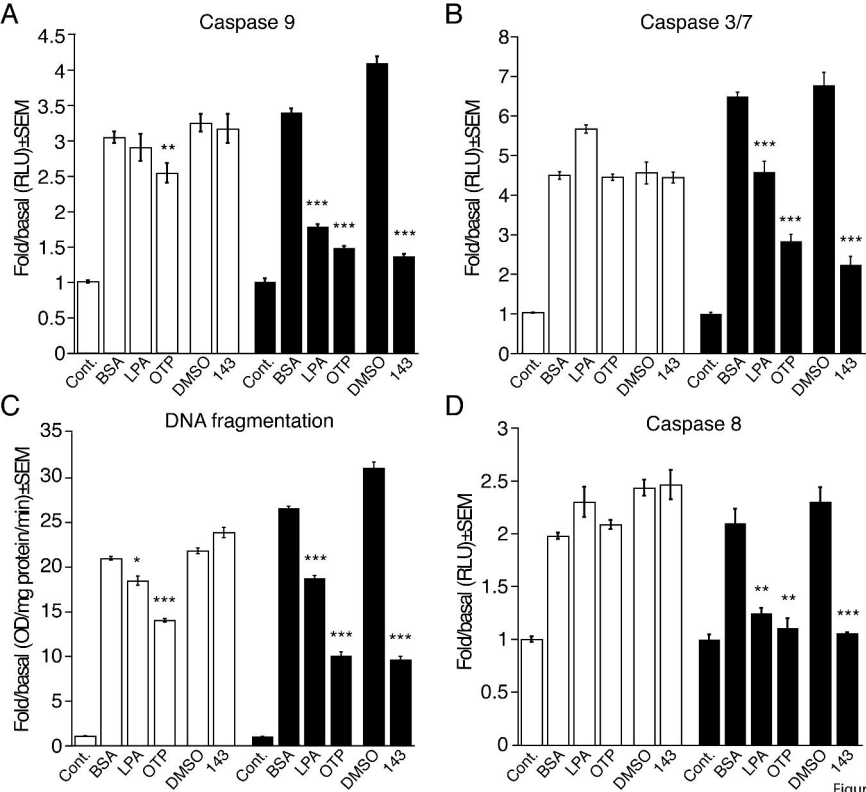


Figure 6

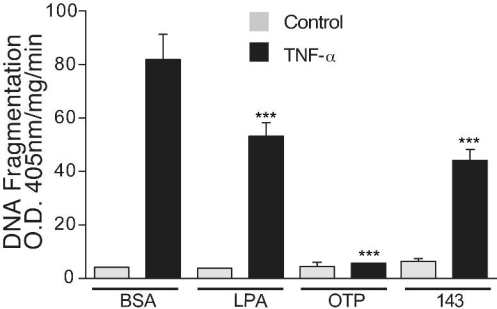


Figure 7

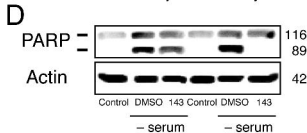
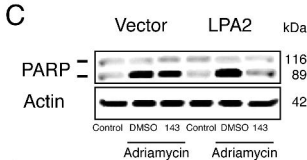
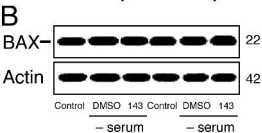
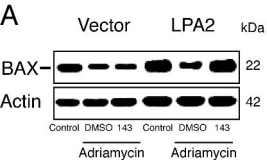


Figure 8

